NASA TECHNICAL MEMORANDUM

NASA TM X-67971

NASA TM X-67971

TEMPORAL SURVEY OF ELECTRON NUMBER DENSITY AND ELECTRON TEMPERATURE IN THE EXHAUST OF A MEGAWATT MPD - ARC THRUSTER

by Charles J. Michels, James R. Rose, and Donald R. Sigman
Lewis Research Center
Cleveland, Ohio

TECHNICAL PAPER proposed for presentation at
Tenth Aerospace Sciences Meeting sponsored by
the American Institute of Aeronautics and Astronautics
San Diego, California, January 17-19, 1972

TEMPORAL SURVEY OF ELECTRON NUMBER DENSITY AND ELECTRON TEMPERATURE IN THE EXHAUST OF A MEGAWATT MPD - ARC THRUSTER

Charles J. Michels, James R. Rose, and Donald R. Sigman
Lewis Research Center
National Aeronautics and Space Administration
Cleveland, Ohio

Abstract

Temporal and radial profiles are obtained 30 cm downstream from the anode for two peak arc currents (11.2 kA and 20 kA) and for various auxiliary magnetic fields (0, 1.0 T, and 2.0 T) using the Thomson scattering technique. Average density and temperature are relatively constant for over 100 microseconds with significant fluctuations. Radial profiles obtained are relatively flat for 4 cm from the axis. Compared to earlier 20 cm data, the exhaust density has decreased significantly (8×10^{13} cm^{-3}), the average temperature (4.6 eV) has not changed, and the density "hole" with an auxiliary magnetic field has enlarged.

Introduction

This report describes the experimental investigation of the electron number density and electron temperature of the exhaust of a single-shot, pulsed, MPD-Arc thruster. This effort is part of a continuing program to investigate megawatt-level MPD-Arc thrusters at Lewis Research Center. This work compliments the lower power level MPD thruster research in providing scaling criteria and early definition of engineering problems. It also provides an understanding of the physical characteristics of the exhaust for those applications that are not thruster oriented; such applications as blow-down reentry simulation tunnels and plasma injectors.

Earlier reported work described the dynamic terminal characteristics[1], the initial examination of exhaust characteristics[2], the progress and interrelation of research on various power level MPD thrusters[3], the initial behavior of a pressure pulse measured in the exhaust[4], and extended pressure history of the exhaust[5].

This report describes an extension of research first reported by Michels and Sigman[2]. In that paper[2], peak values of the electron number density and electron temperature were measured for various engine conditions and various radial locations at an axial distance, Z, 20 cm down the exhaust duct from the face of the thruster anode. In the present paper, the electron number density N_e, and electron temperature, T_e, are determined in the same manner (90°-Thomson scattering using a Q-switched laser light source), but the work is extended to describe the average temporal variation for a period of at least 100 microseconds after plasma arrives at the measuring station. The axial measuring station for this work is at Z = 30 cm.

This attempt to measure the temporal variation of the exhaust was prompted by results obtained by Michels and York[4,5]. In Ref. 4, the starting transient dynamic exhaust pressure was described. It was concluded that the large initial pressure pulse observed was caused by a neutral shock or modified blast wave. The initial exhaust pressure pulse is about 20 microseconds wide, consists mainly of neutral gas, and is followed for the next few hundred microseconds by lower-valued and time-varying exhaust pressure that is caused by flowing plasma. The preliminary description of the time-varying plasma pressure (for the time period of 200 μsec after the initial neutral pressure pulse) is described in Ref. 5. With the exhaust pressure versus time known for the full powering period, other independent measurements of the time-varying exhaust were attempted. This paper is part of that effort. It is hoped that these measurements can be correlated at a later date with detailed plasma pressure measurements.

Apparatus

Plasma Accelerator

A cross-sectional view of the arc chamber is shown in Fig. 1. An iron filings map of the magnetic field is also shown. The cathode is a tungsten ribbon measuring 1 cm wide, 2 cm long, and 1 mm thick. The anode is a 4.2-cm-i.d. copper ring.

Nitrogen propellant is introduced into the arc chamber by a high-speed gas valve that is operated by an electromagnetic actuator. The arc is powered when the cold gas differential pressure across the anode orifice reaches its maximum value. It was previously determined that this condition occurs 650 microseconds after the gas puff is introduced into the arc chamber. At the time the arc is powered the cold gas flow rate is 7 g/sec. The arc is energized by a crowbarred, 10 kilojoule capacitor bank described in Refs. 3 and 6. The arc produces a transient plasma flow into the evacuated glassware section for a few hundred microseconds.

Instrumentation

Thomson Scattering

Figure 2 shows the schematic of the laser diagnostic equipment and its relation to the plasma test section. The laser is a Q-switched ruby with 2 joules output. The 90°, Doppler shifted, Thomson scattered light signal is sensed by the two photomultiplier tubes after having passed through the indicated interference filters[7]. The light stops and beam dumps shown in Fig. 2 serve to minimize the stray light entering the detection system. The broadening of the line shape of the scattered light is due only to electron temperature since in the experiment the scattering parameter [$\alpha = \lambda/(4\pi\lambda_D \sin \theta/2)$] is approximately 0.1. λ is the laser wavelength and λ_D the plasma Debye length. Because the plasma electron velocity distribution is Maxwellian, single-shot data from two filters with different peak wavelengths is sufficient to determine the electron temperature. Using the available transmission curves for the interference filters the fraction of scattered light passed by each filter is calculated as a function of electron temperature. In taking data the ratios of signals from two different filters are computed for

each shot and then a series of ten ratios is averaged before determining the temperature.

The system is calibrated for density by measuring the Rayleigh scattered light when the glass test section is filled with nitrogen at a pressure of a few millimeters Hg. The shot to shot variation in the calibration signals is less than 10 percent.

Results and Discussion

General Comments

When terminal characteristics of the thruster are measured there is a small amount of shot to shot variation. On the other hand, when the exhaust characteristics of the thruster are measured there is significant shot to shot variation. These variations occur even though no evidence of spoking instability[3] is noted and mass flow per shot is held relatively constant. The present experiment, using the Thomson scattering technique displays these variations. The technique has excellent temporal and spatial resolution. Thus the local and temporal variations in number density and electron temperature of the exhaust are detected easily. These variations show up as significant data scatter (large mean deviations). Figure 3 shows this effect clearly. The average value of the electron number density and electron temperature in the exhaust, along with their respective mean deviations, are shown for a particular station, $R = 4$ cm and $Z = 30$ cm, and a particular peak current, 20 kA. Figure 3(a) is for the case of an applied auxiliary magnetic field of 1.0 T while Fig. 3(b) is for the case of no auxiliary magnetic field (self field only).

Each data point of the figure presents the mean value of 10 separate shots. These shots are taken, 10 at a particular time after arc initiation, and span the time interval from approximately 70 microseconds to 200 microseconds. The limit of detectability of the electron number density for the measuring system is 1.0×10^{19} m^{-3}. Any plasma that arrives earlier than the earliest data point in the figure has less density than this detectable limit. The earliest data point times are within a few microseconds beyond that condition. In Fig. 3(a) data are shown beginning at 76 microseconds and continuing up to 200 microseconds. Detectable data exist beyond this time but for practical reasons only about 120 to 130 microseconds of data are gathered. From exhaust pressure histories reported in Ref. 4, it is estimated that the interval of interest should be about that time period.

Typical Data

Figure 3(a) displays the data for an auxiliary magnetic field of 1.0 T, peak arc current of 20 kA, a radial station 4 cm off axis, and an axial station of 30 cm. The mean value of the electron number density for these conditions is surprisingly constant, 8×10^{19} m^{-3}, from 76 to 200 microseconds. The electron temperature ranges from 4 to 6 eV during this time period and the mean deviation is large. Purposely, a curve through the mean values was not attempted, because it would not accurately reflect the temporal behavior of a particular shot.

For the corresponding case with no auxiliary magnetic field (Fig. 3(b)), the electron temperature is lower, 3 to 4 eV, and the mean deviation is lower. This is a lower powered case. At lower temperatures, the ratio of scattered light signal to plasma light signal (signal to noise ratio) is larger. Thus the data is less subject to readibility and interpretation errors. The mean value of the electron number density increases with time for this case. In fact, N_e goes above that for the auxiliary field case shown in Fig. 3(a) about 30 microseconds after the plasma arrives at $Z = 30$ cm, and rises to values of 10 to 12×10^{19} m^{-3}.

Variation With Peak Arc Current

All the data discussed so far are for a peak arc current of 20 kA. If the peak arc current is reduced to 11.2 kA, the data for conditions corresponding to Fig. 3 are lower and have larger mean derivations. In fact, the data for the no auxiliary field case are below the detectable limit at $R = 4$ cm. When the auxiliary magnetic field is increased to 1.0 T, the electron number density is above the detectable limit but the relatively small signal to noise ratio makes the raw data difficult to interpret. This is reflected in the large mean derivations as shown in Fig. 4.

Radial Survey

The preceding data have been for one radial location ($R = 4$ cm). However, data were also taken at two other radial stations ($R = 0$, 2 cm). These radial surveys were performed opposite the laser side of the test section.

The electron number density is above the detectable limit at $R = 0$ and $R = 2$ cm for only two sets of conditions, for which radial profile measurements were attempted. These sets of conditions are for no auxiliary magnetic field at both the high (20 kA) and low (11.2 kA) peak arc current cases.

For a peak arc current of 20 kA and no auxiliary magnetic field data were obtainable at all three radial stations (0, 2 cm, and 4 cm). The profiles of N_e and T_e (not shown) are relatively flat. The temporal behavior of N_e and T_e at $R = 0$ and 2 cm is much like the data shown in Fig. 3(b) for $R = 4$ cm.

When the peak arc current is reduced to 11.2 kA (no auxiliary magnetic field), the electron number density at $R = 4$ cm is below the detectable limit. The profile of N_e and T_e at $R = 0$ and 2 cm (not shown), however, is again relatively flat. The electron number density drops off beyond $R = 2$ cm to some level below the detectable limit at $R = 4$ cm.

Comparison With Earlier Work

The work described in this report is for one axial station, $Z = 30$ cm. This was chosen because other types of probes showed best shot to shot data reproducibility at this station. Earlier work[2] was for a station at $Z = 20$ cm, for only one time point (peak value). The data from Fig. 5 of Ref. 2 are shown again in this report as Fig. 5. The electron number density radial profile at $Z = 30$ cm for no auxiliary magnetic field and a peak arc current of 20.0 kA (Fig. 3(b)) was about an order of magnitude lower (8×10^{19} m^{-3}) than the previous values at $Z = 20$ cm but the shape of the profile is similar to that of Fig. 5. The electron temperature

profile at Z = 30 cm and Z = 20 cm are very similar.

For an auxiliary magnetic field of 1.0 T and a peak arc current of 20.0 kA (Fig. 3(a)), the only detectable data are at R = 4 cm for Z = 30 cm. The number density was again about an order of magnitude less than at Z = 20 cm. The electron temperature was about the same as at Z = 20 cm. The profile was peaked at R = 2 cm for Z = 20 cm and the new data (Fig. 3) shows this peak to have moved out to R = 4 cm. The plasma exhaust profile peak has expanded at Z = 30 cm under the influence of the diverging magnetic field.

Although not shown for an auxiliary magnetic field of 2.0 T and a peak arc current of 20.0 kA, the signal to noise ratio is smaller and the only detectable data is at R = 4 cm for Z = 30 cm. The number density is again about an order of magnitude less than the corresponding data of Fig. 5 (Z = 20 cm data).

Note that the electron temperature (4 to 6 eV) measured are almost the same at Z = 30 cm as those reported earlier for Z = 20 cm. High electron heat conduction in the exhaust could account for this, as pointed out in Ref. 8 in an analysis of plasma expansion in a magnetic nozzle.

Conclusions

The average temporal variation of the electron number density (N_e) and the electron temperature (T_e) in the exhaust of a pulsed megawatt MPD-Arc plasma thruster were determined for two different peak arc-current cases (11.2 kA and 20.0 kA) for various values of auxiliary magnetic field (0.0, 1.0 T and 2.0 T). Radial profiles were obtained for an axial station 30 cm downstream of the anode. The Thomson scattering technique was used and provided high-resolution without the need for auxiliary methods or assumptions.

An average value of N_e and T_e was obtained (for cases above the detectability limit of electron density of 1.0×10^{19} m^{-3}) for each increment of time between detectable plasma arrival and for over 100 microseconds thereafter. The experiment brings out the following facts:

(1) the average values of N_e and T_e are relatively constant over the observed time even though pressure is not constant during the same time period.

(2) There were significant fluctuations in the plasma exhaust. The actual wave forms of temporal variations are not measurable by this technique because of these thruster exhaust fluctuations, low signal levels, background plasma light variations, and the very localized (temporally and spatially) nature of the measurement.

(3) Radial profiles of N_e and T_e were measurable for only two sets of conditions, each with no auxiliary magnetic field. For the 20 kA peak arc current case data were obtained at R = 0, 2 cm, and 4 cm and show relatively flat profiles. The other measurable condition is for the 11.2 kA peak arc current case. Here the N_e and T_e profiles are relatively flat from R = 0 to R = 2 cm, but the data were below the detectable limit at R = 4 cm. The electron number density is lower for the 11.2 kA peak arc current case but the electron temperature was unchanged within the spread of the data. Radial profiles for applied magnetic field of 1.0 T and 2.0 T were not obtainable.

(4) The electron number density decreases by an order of magnitude in the axial distance between 20 cm and 30 cm. The exhaust is expanding significantly in these 10 cm.

(5) When an auxiliary magnetic field of 1.0 T or 2.0 T is applied to the arc there is a "hole" in the electron number density profile. The only detectable data are at R = 4 cm. This "hole" is larger at the Z = 30 cm station than that found in earlier referenced work at a Z = 20 cm station.

(6) Electron temperature measurements are much more sensitive to the fluctuations in the exhaust than are electron number density measurements. Large raw data scatter exists and the method of the data reduction to obtain T_e amplifies the effect of raw data scatter.

(7) The electron temperatures (4 to 6 eV) are almost the same at Z = 30 cm as those reported earlier at Z = 20 cm.

References

1. Michels, C. J., "Dynamic Voltage-Current Characteristics of a Megawatt MPD-ARC Thruster," AIAA Journal, Vol. 9, No. 1, Jan. 1971, pp. 173-176.
2. Michels, C. J. and Sigman, D. R., "Exhaust Characteristics of a Megawatt Nitrogen MPD-ARC Thruster," AIAA Journal, Vol. 9, No. 6, June 1971, pp. 1144-1147.
3. Plasmas and Magnetic Fields in Propulsion and Power Research, SP-226, 1970, NASA, Washington, D.C., pp. 21-22.
4. Michels, C. J. and York, T. M., "Pressure Measurements in the Exhuast of a Pulsed Megawatt MPD-ARC Thruster," Paper 71-196, Jan. 1971, AIAA, New York, N.Y.
5. Michels, C. J. and York, T. M., "Flow Effects in the Exhaust of Megawatt, Transient, Gas-Fed Arc," TM X-67931, 1971, NASA, Cleveland, Ohio.
6. Michels, C. J. and Terdan, F. F., "Characteristics of a 5-Kilojoule, Ignitron-Switched, Fast-Capacitor Bank," TN D-2808, 1965, NASA, Cleveland, Ohio.
7. Patrick, R. M., "Thomson Scattering Measurements of Magnetic Annular Shock Tube Plasmas," Physics of Fluids, Vol. 8, No. 11, Nov. 1965, pp. 1985-1994.
8. Walker, E. L. and Seikel, G. R., "Axisymmetric Expansion of a Plasma in a Magnetic Nozzle Including Thermal Conduction," TN D-6154, 1971, NASA, Cleveland, Ohio.

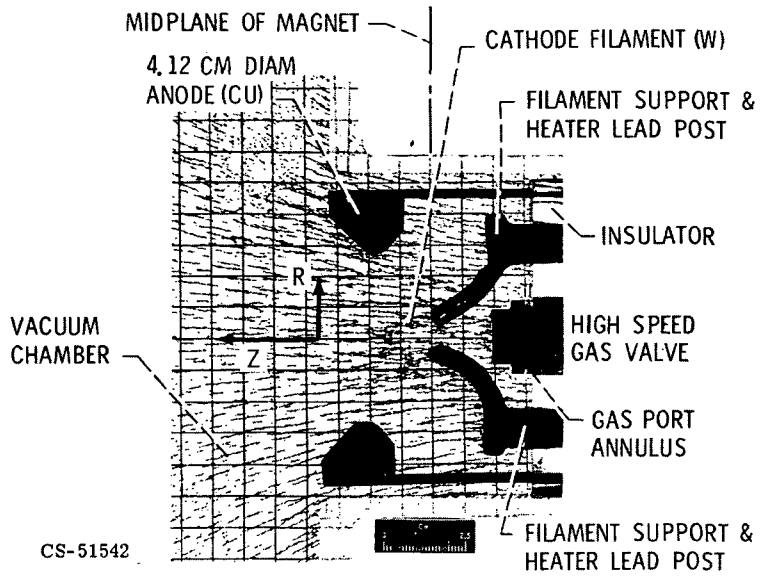

Figure 1. - Arc chamber.

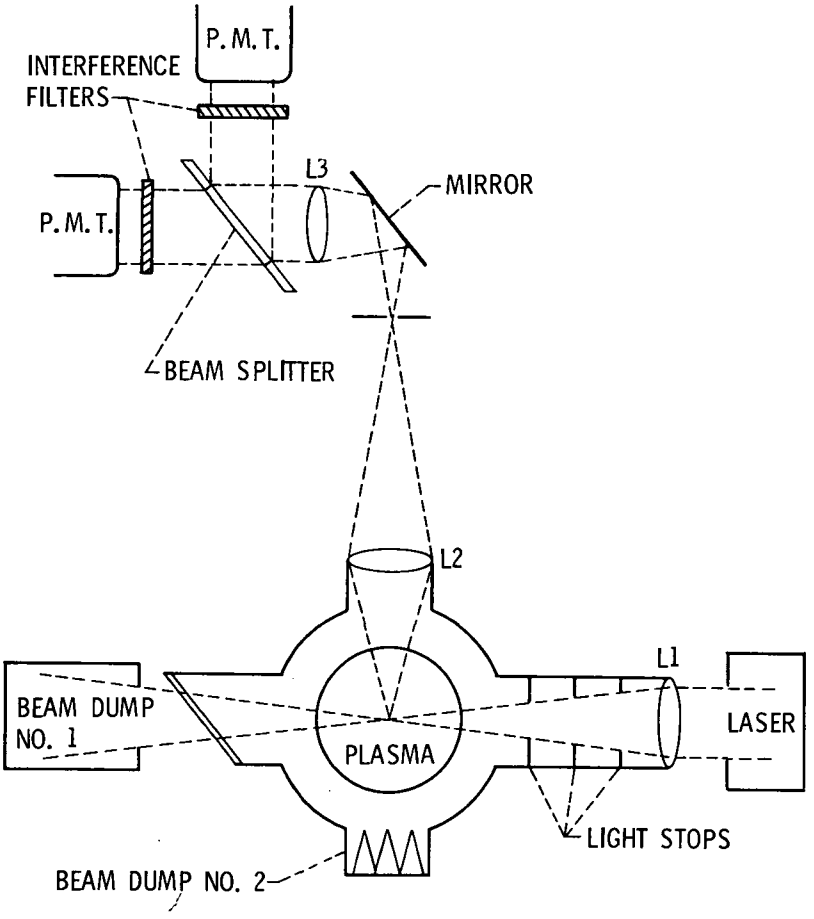

Figure 2. - Schematic of scattering diagnostic equipment.

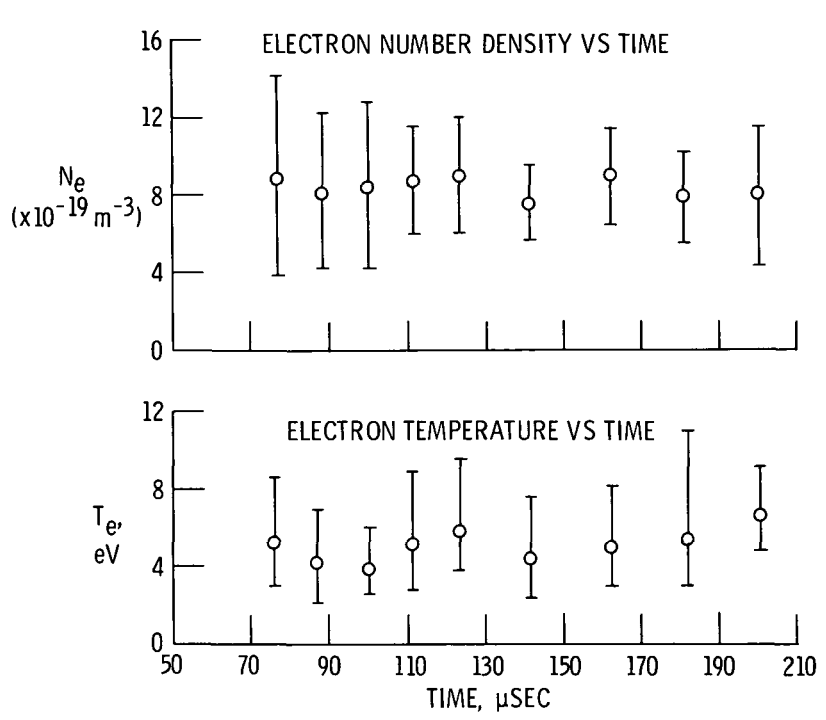

(a) Applied magnetic field case. 20 kA, B = 1.0 T, R = 4 cm, Z = 30 cm.

Figure 3. - Temporal exhaust characteristics.

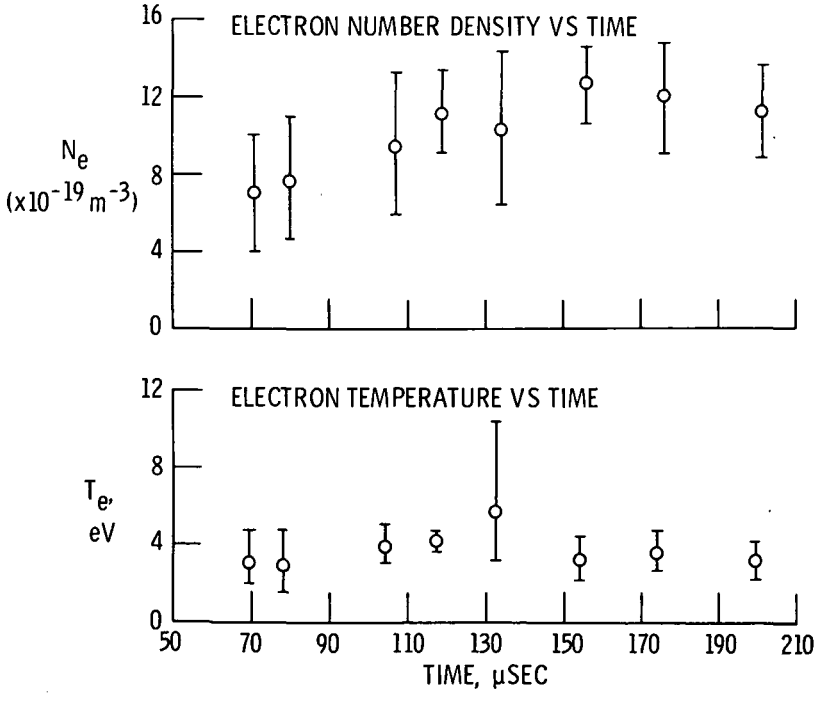

(b) Self-field case. 20 kA, B = 0, R = 4 cm, Z = 30 cm.

Figure 3. - Concluded.

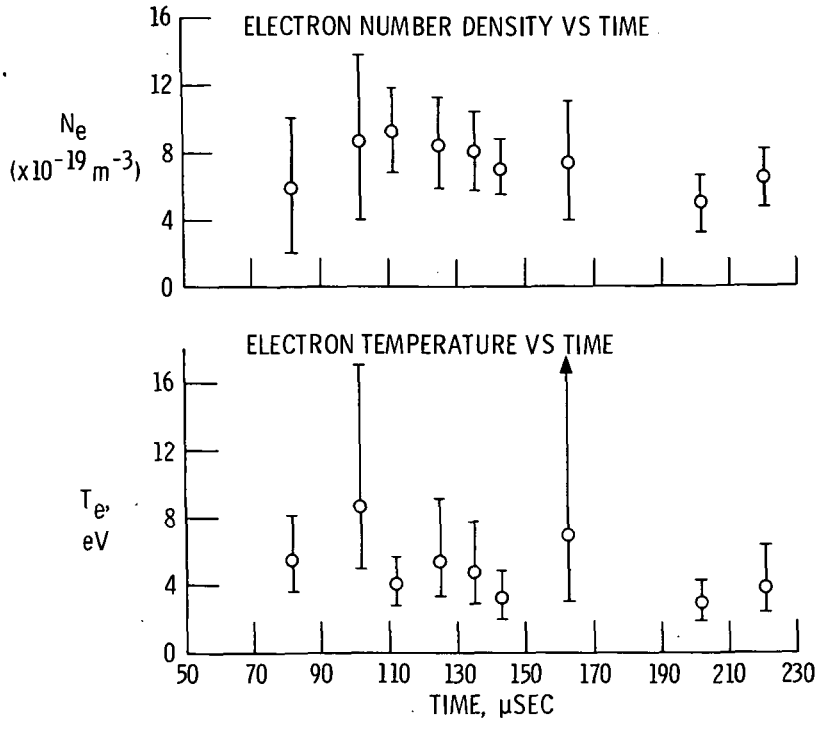

Figure 4. - Temporal exhaust characteristics. (11.2 kA case, B = 1.0 T, R = 4, Z = 30 cm.)

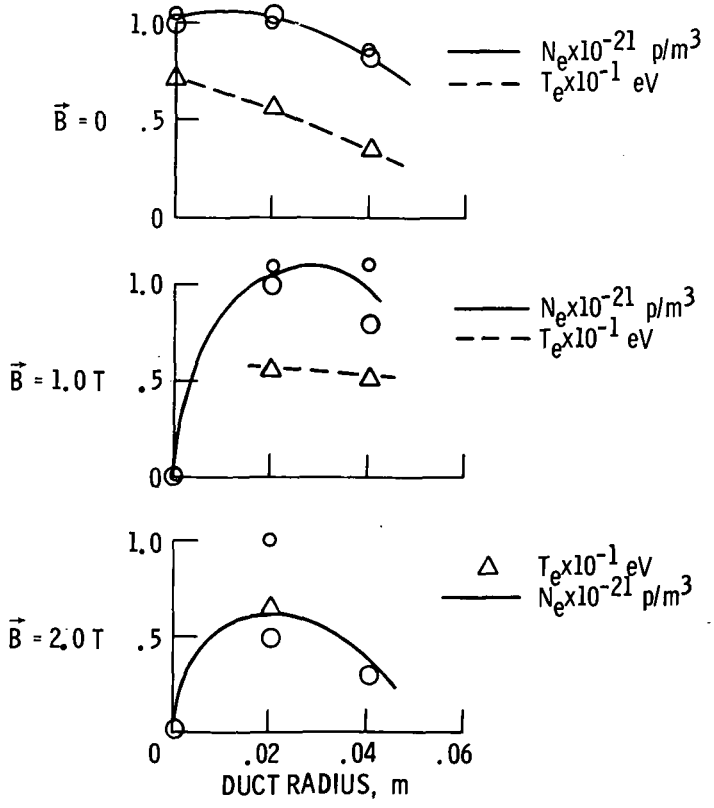

Figure 5. - Exhaust characteristics. 20 kA, Z = 20 cm (data of ref. 2).